Excitonic Fano Resonance in Freestanding Graphene

Dong-Hun Chae*,[1] Tobias Utikal*,[2,1] Siegfried Weisenburger,[2,1] Harald Giessen,[2] Klaus v. Klitzing,[1] Markus Lippitz,[2,1,†] and Jurgen Smet[1,‡]

[1] *Max Planck Institute for Solid State Research, Heisenbergstrasse 1, D-70569 Stuttgart, Germany*
[2] *4th Physics Institute and Research Center SCOPE, University of Stuttgart, Pfaffenwaldring 57, D-70550 Stuttgart, Germany*

(Dated: January 7, 2011)

We investigate the role of electron-hole correlations in the absorption of freestanding monolayer and bilayer graphene using optical transmission spectroscopy from 1.5 to 5.5 eV. Line shape analysis demonstrates that the ultraviolet region is dominated by an asymmetric Fano resonance. We attribute this to an excitonic resonance that forms near the van-Hove singularity at the saddle point of the band structure and couples to the Dirac continuum. The Fano model quantitatively describes the experimental data all the way down to the infrared. In contrast, the common non-interacting particle picture cannot describe our data. These results suggest a profound connection between the absorption properties and the topology of the graphene band structure.

arXiv:1101.1158v1 [cond-mat.mes-hall] 6 Jan 2011

The material properties and the atomic structure of graphene are intimately connected. Most electronic effects can be understood by the unique band structure deduced from a tight-binding model of uncorrelated electrons [1]. A prominent example is the constant optical absorption for photon energies in the infrared wavelength range. It is a consequence of the linear dispersion relation near the K points in the Brillouin zone, the so-called Dirac cones. The absorption is given by fundamental constants alone as the product of the fine structure constant in vacuum $\alpha \approx 1/137$ and π [2,3,4], and it is independent of the velocity of the Dirac fermions. Here, we demonstrate experimentally by line shape analysis that a single-particle model cannot describe the absorption spectrum of freestanding graphene in the visible and ultraviolet spectral region. The saddle point (M) in the band structure (see Fig. 1) causes a van-Hove singularity with a divergent density of states, allowing for a strong optical transition [5]. In this case, electron-hole correlations can lead to effects beyond the single-particle picture. An excitonic resonance at an energy slightly below the van-Hove singularity becomes possible. At a saddle point, the excitonic resonance takes a Fano shape as the discrete exciton state couples to the continuum formed by the band descending from the saddle point [5,6]. In the following we show that the Fano model of the excitonic resonance describes the complete optical spectrum of graphene from the ultraviolet all the way down to the infrared part of the electromagnetic spectrum.

A Fano resonance occurs when a discrete state couples to a continuum of states [6]. The resulting spectrum has the form

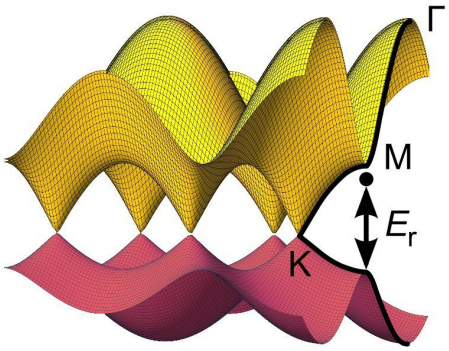

FIG. 1: Electronic band structure of graphene with the saddle point (M) and an illustration of the excitonic state (dot).

$$A_{\mathrm{Fano}}(E) = C\,\left(1 + \frac{q^2-1}{1+s^2} + \frac{2qs}{1+s^2}\right) = C\,\frac{(s+q)^2}{1+s^2} \tag{1}$$

where

$$s = \frac{E - E_r}{\gamma/2} \quad .$$

The damping rate of the resonance at an energy E_r is quantified by the line width γ. The asymmetric spectral shape is determined by the unit-free Fano parameter q, which describes a ratio between the transition probabilities to the discrete level and a state in the continuum. C is an overall scaling factor. The three terms in the bracket may be interpreted as a transition into the continuum, as a Lorentzian associated with the discrete resonance, and as an interference term, respectively [6].

The single particle picture excludes electron-hole correlations. The spectral shape of the interband transition near a saddle point is proportional to the joint density of states. For a saddle point in a two-dimensional system, the joint density of states is given by [5]

$$D(E) \propto -\ln(|E - E_r|) \quad .$$

*These authors contributed equally.
†Electronic address: m.lippitz@physik.uni-stuttgart.de
‡Electronic address: j.smet@physik.uni-stuttgart.de

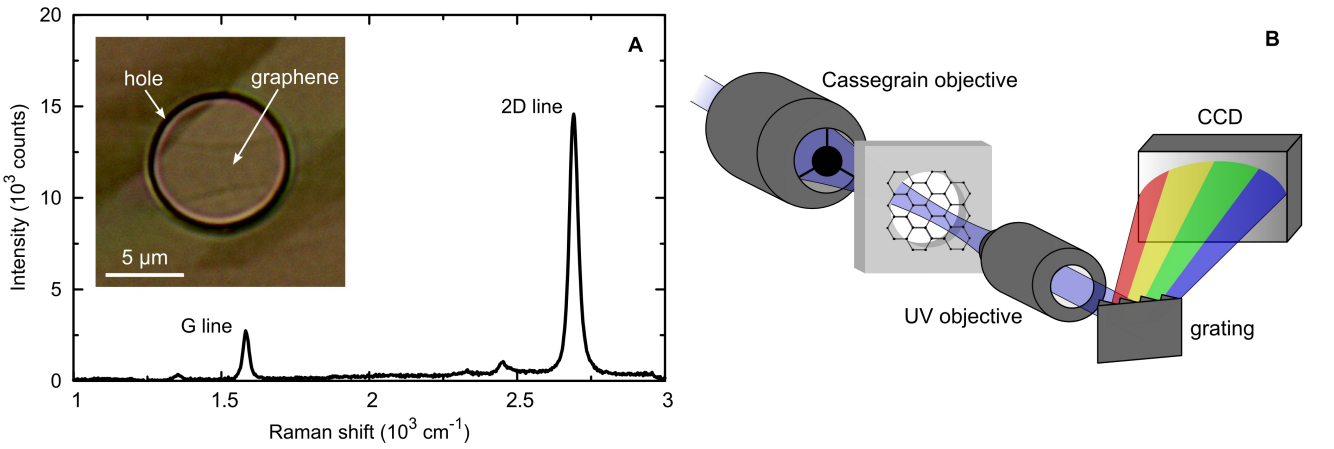

FIG. 2: (**A**) Raman spectrum of a typical freestanding graphene sample. Inset: Optical microscope image of a measured graphene layer. This image was taken in transmission mode. (**B**) Schematic view of the experimental setup.

To take the inhomogeneous broadening into account, we convolute the resulting lineshape with a Gaussian function of variable width γ. The constant absorption stemming from the Dirac cones is modeled as a constant offset B. The alternative single-particle model is thus given by

$$A_{\mathrm{singleparticle}}(E) = \qquad (2)$$
$$C\left(B + \exp\left[-\frac{(E-E_r)^2}{\gamma^2}\right] \otimes [-\ln(|E-E_r|)]\right) \quad ,$$

where $\otimes$ denotes a convolution. Note that both models have the same number of free parameters.

Our samples are freestanding graphene monolayer and bilayer. The samples are fabricated by transferring graphene from a silicon substrate to an aperture in a polymer resist (see Fig. 2A inset). The graphene flakes are first prepared on an oxidized silicon substrate using mechanical exfoliation of natural graphite. Graphene and bilayer graphene are identified by the optical contrast in a microscope image [7] and by Raman spectroscopy [8]. The samples are spin-coated with a 500 nm thick layer of poly(methyl methacrylate) (PMMA). Disk shapes with a diameter of 8 µm are written on top of the flakes using electron beam lithography. After development, the PMMA layer with the 8 µm aperture together with the graphene flake are removed from the substrate by etching the silicon dioxide in a 5 % NaOH aqueous solution at 90 °C.

We characterize our samples by Raman spectroscopy. Figure 2A shows a Raman spectrum of a typical freestanding graphene sample. The symmetric 2D line at about 2700 cm^{-1} is the hallmark of a monolayer [8]. The position of the G line at approximately 1582 cm^{-1} suggests a negligible level of doping [9] and marginal strain [10] introduced during sample fabrication.

We measure the optical transmission of freestanding monolayer and bilayer graphene in a confocal microscope. Figure. 2B depicts a schematic of the experimental setup. The light source combines a tungsten halogen bulb and a deuterium lamp. We implement point illumination by using the end-face of an optical quartz fiber as a confocal pinhole. The light is then focused onto the sample by an all-reflective Cassegrain objective (Davin Optronics, 74x) with a numerical aperture (NA) of 0.65. A UV microscope objective (Zeiss Ultrafluar, 100x, NA 1.2) recollects the transmitted light which is then directed to the spectrometer, consisting of a monochromator and a liquid nitrogen-cooled CCD camera as detector. Note that we use the Ultrafluar objective without glycerol immersion in contrast to its specifications.

This assembly allows us to take spectra over a photon energy range from 1.5 eV to 5.5 eV with a spatial resolution on the sample better than 1.5 µm. Due to the limited spectral bandwidth of each spectrometer grating, the whole spectrum is measured by concatenating data from three exposures using two different gratings. The spectral resolution is about 10 meV.

The transmittance T is determined by the ratio of the transmitted light intensity through the graphene membrane to the transmitted intensity when the layer is replaced by an empty reference aperture nearby. The transmittance for bilayer graphene is measured in the same way. The weak absorption of the mono-atomic film implies a negligible reflectance, hence the absorbance A can be written as $A = 1 - T$.

An example for the absorption spectra acquired in this way is given in Figure Fig. 3A. For low photon energies, the spectra are almost flat. The limiting values are close to integer multiples of $\pi\alpha$ in accordance with published results [3]. At higher energies, we find an asymmetric peak at about 4.5 eV, as indicated by previous ellipsometric measurements [11,12]. The Fano model, eq. (1), excellently describes our experimental data for both monolayer as well as bilayer graphene over the entire recorded spectral range. The single particle picture in a two-dimensional system results in a symmetric fit function, eq. (2). It utterly fails to describe the measured spectra (Fig. 3B, dashed line). In accordance with

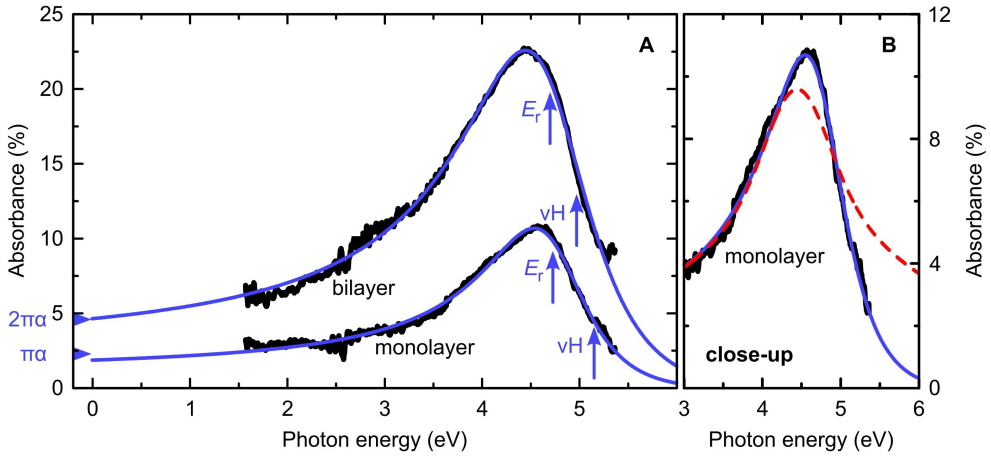

FIG. 3: (A) Absorbance (= 1 - Transmittance) spectra of freestanding monolayer and bilayer graphene (black thick lines) are well described by a Fano model (blue thin lines). The difference between the resonance energy E_r and the van-Hove singularity (vH) determines the exciton binding energy. (B) Close-up of the monolayer spectrum (black thick line) with the Fano fit (blue thin line) compared to a model neglecting electron-hole correlations (red dashed line).

ab initio calculations [13], the excitonic resonance carries all the oscillator strength. The direct interband transition cannot be identified.

The Fano model yields the excitonic resonance positions E_r for monolayer and bilayer graphene (Table I). The exciton binding energy is the energetic difference from the resonance to the van-Hove singularity calculated in the single-particle picture [13]. We find binding energies of about 400 meV and 250 meV for monolayer and bilayer graphene, respectively. Table I summarizes the resulting fit parameters and characteristic deduced values. For common three-dimensional bulk metals, static screening by the electrons would prevent correlated electron-hole pairs within the Thomas-Fermi approximation. A reduced dimensionality, however, such as in one-dimensional metallic carbon nanotubes weakens the static screening so that excitonic correlations can occur [14]. The screening depends on the density of states near the Fermi energy. For the semi-metallic graphene, the density of states vanishes at the Dirac point and then grows linearly [15]. In bilayer graphene, however, the density of states is constant and nonzero near the Dirac point. For Fermi energies near the Dirac point, the screening ability of electrons in monolayer graphene is therefore hampered, and it is larger in bilayer graphene. As a result, the exciton binding energy is expected to be smaller when comparing bilayer with monolayer graphene in agreement with our measurements.

It is intriguing that the Fano model describes the absorption quantitatively correct over such a broad spectral range. It even reproduces the absorption of $\pi\alpha$ in the low energy limit. According to the Fano model, less than half of the absorption at low energies is due to the constant continuum contribution associated with the Dirac cones. The tail of the excitonic resonance still dominates at these low energies. The success of the single resonance Fano model together with the independence of the low energy absorption limit on the slope of the Dirac cone [2,3] suggests that the detailed shape of the band structure is less relevant, but rather the specific topology of the monolayer and bilayer graphene band structure is crucial.

dataset	E_r (eV)	γ (eV)	q	C (%)	$A(0)/(\pi\alpha)$	E_b (meV)
monolayer*	4.73	1.30	-3.3	0.9	0.82	420
monolayer	4.78	1.58	-3.6	0.7	0.75	370
bilayer*	4.70	1.63	-3.2	2.0	2.0	270
bilayer	4.73	1.39	-3.3	1.8	1.7	240

TABLE I: Summary of the fitting parameters and deduced values. The datasets marked with a star (*) are shown in Figure 3. $A(0)$ denotes the absorbance at zero energy as given by the model, which has to be compared to integer multiples of $\pi\alpha$. E_b is the exciton binding energy calculated as the difference of E_r to the saddle point.

We thank Th. Basché for the loan of the Ultrafluar objective and S. Hein for visualizations.

References

1. A. H. Castro Neto et al., *Rev. Mod. Phys.* **81**, 109 (2009).
2. A. B. Kuzmenko et al., *Phys. Rev. Lett.* **100**, 117401 (2008).
3. R. R. Nair et al., *Science* **320**, 1308 (2008).
4. K. F. Mak et al., *Phys. Rev. Lett.* **101**, 196405 (2008)
5. P. Y. Yu, M. Cardona, *Fundamentals of Semiconductors* (Springer, Berlin, 2005).
6. J. C. Phillips, *Excitons* in J. Tauc (ed.) *The Optical Properties of Solids* (Academic Press, New York, 1966)
7. K. S. Novoselov et al., *Science* **306**, 666 (2004).
8. A. C. Ferrari et al., *Phys. Rev. Lett.* **97**, 187401 (2006).

9. J. Yan et al., *Phys. Rev. Lett.* **98**, 166802 (2007).
10. Z. H. Ni et al., *ACS Nano* **2**, 2301 (2008).
11. V. G. Kravets et al., *Phys. Rev. B* **81**, 155413 (2010)
12. J. W. Weber et al., Appl. Phys. Lett. 97, 091904 (2010).
13. L. Yang et al. , *Phys. Rev. Lett.* **103**, 186802 (2009).
14. F. Wang et al., *Phys. Rev. Lett.* **99**, 227401 (2007).
15. T. Ando, *J. Phys. Soc. Jpn.* **75**, 074716 (2006).